THE JOURNAL OF BIOLOGICAL CHEMISTRY VOL. 287, NO. 12, pp. 8737–8745, March 16, 2012


# Constitutive NADPH Oxidase 4 Activity Resides in the Composition of the B-loop and the Penultimate C Terminus*[S]

Received for publication, December 12, 2011, and in revised form, January 17, 2012 Published, JBC Papers in Press, January 25, 2012, DOI 10.1074/jbc.M111.332494

**Katharina von Löhneysen[‡], Deborah Noack[‡], Patti Hayes[§], Jeffrey S. Friedman[‡], and Ulla G. Knaus[§1]**

*From the [§]Conway Institute, School of Medicine and Medical Science, University College Dublin, Dublin 4, Ireland and the [‡]Scripps Research Institute, Department of Molecular and Experimental Medicine, La Jolla, California 92037*

**Background:** Reactive oxygen species generated by NADPH oxidases are critical second messengers.
**Results:** Unique motifs in the B-loop and C terminus are essential for Nox4 catalytic activity.
**Conclusion:** The active conformation of the Nox4-p22$^{phox}$ complex is dependent on discrete motifs and precise spacing.
**Significance:** Improved understanding of the inactive *versus* the active conformation of Nox enzymes will aid inhibitor development.

**Redox regulation of signaling molecules contributes critically to propagation of intracellular signals. The main source providing reactive oxygen species (ROS) for these physiological processes are activated NADPH oxidases (Nox/Duox family). In a pathophysiological context, some NADPH oxidase complexes produce large amounts of ROS either as part of the antimicrobial immune defense or as pathologic oxidative stress in many chronic diseases. Thus, understanding the switch from a dormant, inactive conformation to the active state of these enzymes will aid the development of inhibitors. As exogenously expressed Nox4 represents the only constitutively active enzyme in this family, analysis of structural determinants that permit this active conformation was undertaken. Our focus was directed toward a cell-based analysis of the first intracellular loop, the B-loop, and the C-terminus, two regions of Nox family enzymes that are essential for electron transfer. Mutagenesis of the B-loop identified several unique residues and a polybasic motif that contribute to the catalytic activity of Nox4. By using a multifaceted approach, including Nox4-Nox2 chimeras, mutagenesis, and insertion of Nox2 domains, we show here that the penultimate 22 amino acids of Nox4 are involved in constitutive ROS generation. The appropriate spacing of the C-terminal Nox4 sequence may cooperate with a discrete arginine-based interaction site in the B-loop, providing an intrinsically active interface that could not be disrupted by peptides derived from the Nox4 C-terminus. These results indicate that accessibility for a Nox4-specific peptide inhibitor might be difficult to achieve *in vivo*.**

NADPH oxidases comprise a family of multimeric membrane-bound enzymes that form reactive oxygen metabolites by reducing molecular oxygen. Interest in these enzymes increased exponentially after the discovery of novel Nox/Duox isoforms with distinct tissue distribution and an apparent role in the pathogenesis of diseases characterized by excessive ROS[2] production. Seven mammalian oxidases, Nox1–5 and Duox1–2, have been identified (1–3). Maturation of the membrane-bound electron transfer complexes, with the exception of Nox5, requires dimerization of the Nox protein with different subunits like p22$^{phox}$, DuoxA1, or DuoxA2. Nox isoforms 1–3 attain catalytic activity by a subsequent assembly process involving additional subunits. Further steps essential for activation can include phosphorylation of the Nox/Duox complex or of regulatory proteins, the binding of calcium to EF-hand motifs and the activation of Rac GTPases. The overall process of superoxide generation is conserved in the "Nox" domain, which contains similarly spaced, highly homologous membrane segments harboring two hemes and incorporates several cofactor binding domains in the cytosolic region. In short, active Nox/Duox complexes catalyze the electron transfer from NADPH to FAD via heme to molecular oxygen, leading to the initial formation of superoxide. Some oxidases, namely Nox4 and Duox1–2, only release $H_2O_2$ as the final product of this reaction, formed by a yet unknown process that appears to reside in the spatial arrangement of the transmembrane domains and/or extracellular loops (4, 5). Nox4 is also unique in its ability to generate $H_2O_2$ constitutively when exogenously expressed (6). In contrast, tight spatiotemporal regulation is usually a hallmark for the other NADPH oxidase family members. Thus, together with the apparent absence of cytosolic regulators, the Nox4-p22$^{phox}$ complex represents a Nox enzyme in its active structural conformation, providing an ideal model to assess which domains or individual amino acid residues contribute to catalytic activity.

The Nox domain is comprised of cytosolic N and C termini separated by six putative transmembrane regions. This arrangement leads to a configuration of three extracellular (A, C,

* This work was supported, in whole or in part, by National Institutes of Health Grant 1RO1 DK080232 (to J. S. F.). This work was also supported by Science Foundation Ireland award (to U. G. K.).

[S] This article contains supplemental Figs. 1–3.

The amino acid sequences of these proteins can be accessed through the NCBI Protein Database under NCBI accession numbers NP_058627.1, XP_003313305.1, NP_001124912.1, XP_001105410.1), XP_002699078.1, XP_003357282.1, XP_001489181.1, XP_002927888.1, NP_056575.1, NP_445976.1, XP_542262.3, NP_001095299.1, FAA00342.1, NP_001029001.1, NP_000388), NP_008983, and NP_056533.

[1] To whom correspondence should be addressed: Conway Institute, University College Dublin, Belfield, Dublin 4, Ireland. Tel.: 353-1-7166719; Fax: 353-1-7166710; E-mail: Ulla.Knaus@ucd.ie.

[2] The abbreviations used are: ROS, reactive oxygen species; HVA, homovanillic acid; PI(4,5)$P_2$, phosphatidylinositol 4,5-bisphosphate.

E) and two intracellular (B, D) loops. Previous reports linked the Nox2 B-loop to the assembly process by providing a binding site for the oxidase component $p47^{phox}$ (7, 8). Mutagenesis of two adjacent arginines in the B-loop abolished superoxide generation in an X-CGD PLB-985 cell model and inhibited membrane translocation of cytosolic proteins $p47^{phox}$ and $p67^{phox}$ (9). The Nox2 B-loop was also targeted by rational design of a cell-permeable peptide that may prevent Nox2 assembly *in vivo*. This peptide, termed Nox2ds-Tat, attenuated ROS generation in the vasculature and had beneficial effects in several animal models of cardiovascular disease (10–13). The partial sequence homology of Nox2ds-Tat with B-loop sequences of other Nox isoforms expressed in the vasculature prevented these effects from being exclusively assigned to Nox2. However, recent studies confirmed the selectivity of Nox2ds-Tat as a Nox2 inhibitor *in vitro* (14). Targeting the constitutive activity of Nox4 selectively by a similar approach might be beneficial in Nox4-mediated pathologies, including fibrosis, tumor progression, or diabetes. Analysis of charged amino acids common in Nox1–4 suggested that B-loops provide an electrostatic interface that is critically involved in electron transport. This interface could either connect to oxidase regulatory proteins, or as recently shown, to the NADPH-FAD-containing dehydrogenase domain in the Nox C terminus (15).

While the B-loops of all Nox isoforms seem to be essential for catalytic activity, the permanently active conformation of Nox4 suggests a unique tertiary structure that is accomplished by distinct sequence motifs. In this study, we analyzed the differences between the Nox2 and Nox4 B-loops and which role the enhanced polybasic charge localized in this region of Nox4 plays. To identify the potential interface between the B-loop and the C terminus, we made use of our earlier observation that the last 22 amino acid residues of Nox4 are required for catalytic activity. By replacing amino acids or inserting a short, unique Nox2-derived sequence, this C-terminal region was probed for Nox4-specific features that determine its catalytic activity. This approach led to the identification of several novel motifs and a discrete polybasic binding site in the B-loop that cannot be disrupted by Nox4-derived peptides.

## EXPERIMENTAL PROCEDURES

*Cell Lines and Cell Culture*—COS-$p22^{phox}$ cells were cultured in DMEM (16). All growth media was obtained from Invitrogen and supplemented with 10% fetal bovine serum.

*Plasmids and Transfections*—hNox4 expression plasmids pcDNA3.0-Nox4, V5-Nox4*wt*, catalytically inactive Nox4 (KD), and Nox4/Nox2 chimera 41b were described previously (4, 6). Amino acid exchange mutations in the B-loop of V5-Nox4, termed MCRN, AY/SF, QAVA, DKNL, DKER, DKDR, DKNR, TRV, RRV, RRE, RRD and KKTKK, as well as changes in the C-terminal region after amino acid 554, termed KTLSK, KTLAK, SAGTR, SYGAR, GVHFIF, GVHFEY, FIF, FEY, and FIY, were generated using the PCR-based QuikChange site-directed mutagenesis kit (Stratagene) according to the manufacturer's protocol. Two peptides corresponding to the Nox4 C terminus, $^{304}$Nox4$^{578}$ and $^{554}$Nox4$^{578}$, were amplified by PCR and inserted into pRK5-GST to generate GST-tagged peptides. Resulting plasmids were verified by sequencing. The plasmids HA-PIP5KI$\alpha$ (WT) and HA-PIP5KI$\alpha$ D309N R427Q (KD) as well as pEGFP-N2-SopB 58–563 (WT) and pEGFP-N2-SopB 58–563 C460S (KD) were kindly provided by Richard Anderson, University of Wisconsin-Madison, and Jorge Galan, Yale University, respectively. Transient transfections of COS-$p22^{phox}$ cells were performed using Lipofectamine Plus (Invitrogen), FuGENE HD (Roche) or FuGENE 6 (Roche) according to the manufacturers' instructions. Briefly, COS-$p22^{phox}$ cells were plated at a density of $1.5 \times 10^5$ cells/well on a 6-well plate. Cells were transfected at 70% confluency with 0.1–4 $\mu$g of plasmid DNA. Experiments were performed 48 h post-transfection.

*Sequence Alignments*—Sequence alignments of Nox4 proteins from different species were generated by Clustal/MAFFT. Sequences aligned were as follows (species, NCBI reference sequence number): NADPH oxidase 4 isoform a (*Homo sapiens*, NP_058627.1); predicted: NADPH oxidase 4 (*Pan troglodytes*, XP_003313305.1), NADPH oxidase 4 (*Pongo abelii*, NP_001124912.1); predicted: NADPH oxidase 4 isoform 3 (*Macaca mulatta*, XP_001105410.1); predicted: NADPH oxidase 4 (*Bos taurus*, XP_002699078.1); predicted: NADPH oxidase 4 isoform 2 (*Sus scrofa*, XP_003357282.1); predicted: NADPH oxidase 4 isoform 1 (*Equus caballus*, XP_001489181.1); predicted: NADPH oxidase 4-like isoform 1 (*Ailuropoda melanoleuca*, XP_002927888.1), NADPH oxidase 4 (*Mus musculus*, NP_056575.1), NADPH oxidase 4 (*Rattus norvegicus*, NP_445976.1); predicted: NADPH oxidase 4 (*Canis lupus familiaris*, XP_542262.3), NADPH oxidase 4 (*Gallus gallus*, NP_001095299.1), TPA, predicted: NADPH oxidase-4 (*Takifugu rubripes*, FAA00342.1) and NADPH oxidase 4 (*Ciona intestinalis*, NP_001029001.1).

*Antibodies and Western Blot Analysis*—Cells were lysed in radioimmune precipitation assay buffer (50 mM Tris (pH 7.4), 100 mM NaCl, 1% Nonidet P-40, 0.1% SDS) containing complete protease inhibitors (Roche). Lysates were clarified by centrifugation at 15,000 rpm for 10 min at 4 °C. Proteins were separated on a 13% SDS-PAGE and electroblotted onto nitrocellulose (Bio-Rad). Membranes were blocked in PBS containing 1.5% BSA and 2% goat serum. Primary antibodies were as follows: anti-Nox4 antibody (17), anti-$p22^{phox}$ antibody FL-195 (Santa Cruz Biotechnology, Santa Cruz, CA), anti-actin (Sigma), anti-HA (Covance), anti-GFP (Millipore) and mAb anti-V5 (Sigma). Secondary antibodies used were goat anti-mouse or goat anti-rabbit conjugated to horseradish peroxidase (Southern Biotech), followed by detection with ECL (Pierce). Alternatively, we used the Odyssey® infrared fluorescence imaging system (LI-COR Biotechnology), blocking with casein blocking buffer and secondary antibodies IRDye 800 goat anti mouse IgG (H + L) 800CW and IRDye 680 goat anti-rabbit IgG (H + L) (LI-COR). Blots were analyzed using Odyssey software.

*Flow Cytometry*—Cells were trypsinized and washed in PBS containing 1.5% BSA and 2% goat serum, incubated with anti-Nox4 antibody or mAb anti-V5 in cold FACS buffer (PBS, 0.5% BSA) on ice for 30 min. For intracellular staining cells were incubated with 0.2% saponin for 10 min on ice prior to antibody incubation. Subsequent to washing in FACS buffer, cells were incubated with secondary antibodies, goat anti rabbit-biotin, or goat anti mouse-biotin (BD Biosciences), followed by washing

and incubation with streptavidin-phycoerythrin (BD Bioscience, NJ). After the final washing step, fluorescence of cells was analyzed using a BD LSR II flow cytometer and FACSDiva 6.0 (BD Biosciences). Cell populations were gated for live cells. Data were analyzed with FlowJo (Tree Star). Untransfected COS-p22$^{phox}$ cells served as negative control.

*ROS Production*—$H_2O_2$ production was measured by monitoring homovanillic acid (HVA) fluorescence as described previously (6). In short, cells were washed with Hanks' balanced salt solution and incubated at 37 °C for 1 h in HVA solution (100 mM HVA, 4 units/ml horseradish peroxidase in Hanks' balanced salt solution with $Ca^{2+}$ and $Mg^{2+}$). The reaction was halted by addition of stop buffer (0.1 M glycine/0.1 M NaOH (pH 12) and 25 mM EDTA in PBS). Fluorescence was read on a Biotek Synergy HT (320 nm excitation, 420 nm emission). Fluorescence readings were converted into nmol $H_2O_2$ on the basis of an $H_2O_2$ standard curve.

*Statistical Analysis*—All experiments were performed at least three times in triplicate (the *error bars* indicate mean ± S.D., $n = 3$). Shown are representative examples of at least three independent experiments. When indicated, an unpaired Student's *t* test was performed. Statistical significance is indicated on the bar graphs: *, $p \leq 0.05$; **, $p \leq 0.01$; and ***, $p \leq 0.001$; comparing the mutant to Nox4*wt*.

## RESULTS

*Nox4 Catalytic Activity is Sensitive to Amino Acid Substitution in the N-terminal Region of the B-Loop*—The first intracellular loop of Nox-type NADPH oxidases is essential for the catalytic activity, *i.e.* ROS generation, and cannot, as demonstrated for Nox2 and Nox4, be replaced by the B-loop of a related Nox enzymes (Fig. 1*A*) (4). Amino acid sequence alignment of Nox B-loops indicates three subregions where two conserved regions flank a highly variable central region (15). The conserved regions are not identical in Nox isoform amino acid composition, and, thus, we asked if substitution of Nox4 residues with residues that are present in Nox2 at the same position would alter Nox4 activity. Nox4-specific B-loop amino acid residues close to the second transmembrane domain that may either represent phosphorylation sites or carry charge were chosen for replacement with residues present in Nox2 (Fig. 1*B*). The proline residue at position 90 in Nox4 was substituted with a non-polar amino acid (alanine) rather than introducing a polar cysteine, the corresponding amino acid in Nox2. The three Nox4 mutants MCRN (T78N), AY/SF (A81S and Y82F) and QAVA (K88A and P90A) were compared with the Nox4 wild-type enzyme after expression in COS7 cells stably expressing human p22$^{phox}$ (COS-p22$^{phox}$). Equivalent expression of Nox4 and Nox4 mutants was detected in immunoblots probed with a Nox4 antibody that recognizes the extracellular E-loop. In contrast, $H_2O_2$ production was reduced to ~50% in all mutants when compared with wild-type Nox4 (Fig. 1*C*). Earlier studies showed that Nox4-mediated $H_2O_2$ release into the medium of adherent COS-p22$^{phox}$ cells correlates with translocation of a functional Nox4-p22$^{phox}$ complex to the plasma membrane (4). Flow cytometry of non-permeabilized cells transfected with Nox4wt or Nox4 mutants revealed localization

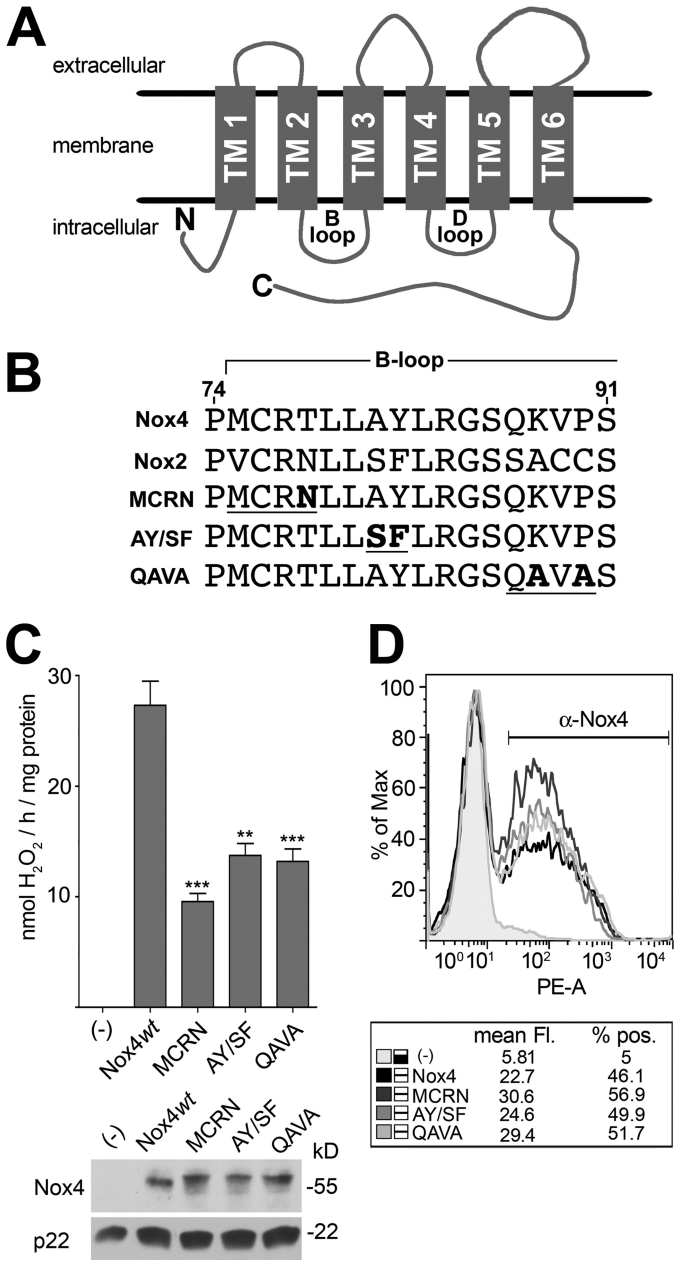


FIGURE 1. **Substitution of N-terminal B-loop residues in Nox4 impairs ROS generation.** *A*, simplified model of Nox4 with B- and D-loops located intracellularly. *B*, sequence alignment of Nox4*wt*, Nox2*wt*, and the Nox4 mutants MCRN, AY/SF, and QAVA. Numbers refer to the amino acid position in Nox4*wt*. Changed amino acids are in *boldface*. *C*, COS-p22$^{phox}$ cells transfected with Nox4*wt* or indicated Nox4 mutants were tested for $H_2O_2$ generation. Expression of Nox proteins was analyzed by immunoblotting using p22$^{phox}$ as a loading control. *D*, flow cytometry analysis of cell surface expression of Nox4*wt* and mutants by staining with anti-Nox4 antibody. Fluorescence of whole-cell populations (phycoerythin-label acquisition, *PE-A*) is calculated as geometric mean. The gate was set to include 5% of control cells. COS-p22$^{phox}$ cells (-) served as a control for *B–D*.

of all Nox4 proteins on the cell surface (Fig. 1*D*) (supplemental Fig. 1).

*Introduction of a Negative Charge in the C-Terminal Region of the Nox4 B-Loop is Detrimental to Enzyme Activity*—The sequence D*X*NL (*X* indicates a polar, basic residue) of the conserved C-terminal region in the Nox1–3 B-loops is substituted to D*X*SR in Nox4 (Fig. 2*A*). Changing the Nox4 sequence into

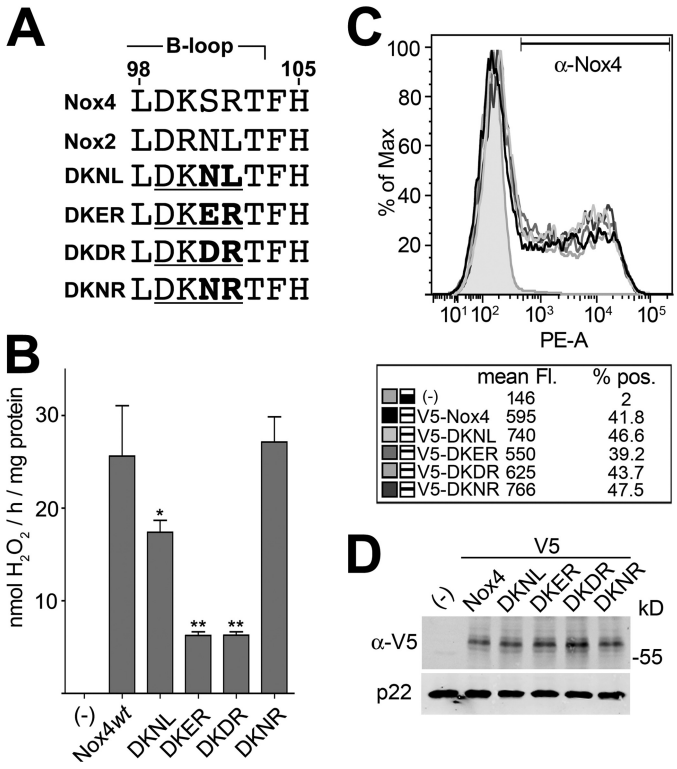


FIGURE 2. **The Nox4 C-terminal B-loop is sensitive to replacement with acidic residues.** *A*, sequence alignment of amino acid composition of Nox4*wt*, Nox2*wt*, and the Nox4 B-loop mutants DKNL, DKER, DKDR, and DKNR. The numbers refer to the amino acid position in Nox4*wt*, and mutated amino acids are in *boldface*. COS-p22$^{phox}$ cells transiently transfected with V5-tagged Nox4*wt* or indicated Nox4 mutants were tested for $H_2O_2$ generation by HVA (*B*) and cell surface localization by flow cytometry (*C*). Fluorescence is calculated as geometric mean, and the gate was set to include 2% of control cells. Expression was monitored by immunoblotting using p22$^{phox}$ as a loading control (*D*). COS-p22$^{phox}$ cells (-) served as a control for *B–D*.

D*X*NL or into D*X*NR does not alter the catalytic activity of Nox4 substantially (Fig. 2*B*). In contrast, introducing a negative charge into the D*X*SR sequence, such as D*X*ER or D*X*DR, reduces ROS generation substantially (Fig. 2*B*). Thus, the Nox4 D*X*SR sequence is required for yet unknown interactions that will be disrupted by introducing additional negative charge. Still, this sequence will tolerate replacement with different polar, uncharged amino acids. The Nox4 D*X*SR mutants showed comparable expression and cell surface localization (Fig. 2, *C* and *D*).

*The RRTRR Motif in the B-Loop Is Required for ROS Production by Nox4*—The variable region of the Nox4 B-loop differs from other Nox enzymes by the presence of a motif where two arginines are separated by a threonine residue from two further arginines. Previous studies revealed the importance of the second pair of basic amino acid residues in this motif that are conserved in Nox1–4 (9, 15). As the first arginine in Nox4 RRTRR, Arg-92, is not conserved in Nox2, we mutated this residue to the threonine residue present in Nox2. Likewise, the Nox4 threonine residue separating the sets of arginines was replaced by valine to mimic the Nox2 sequence (Fig. 3*A*). Changing the Nox4 RRTRR motif into Nox2 TRVRR reduced ROS generation of mutant Nox4 TRV to 25% of the wild-type Nox4 output. Single mutation of the Nox4 wild type into Nox4 T94V indicated that amino acid Arg-92 but not the Val-94 residue is required for Nox4 activity. The highly positive charge in the RRTRR sequence is maintained when replacing the polar threonine with a non-polar valine residue but would be disrupted by a negatively charged amino acid. Thus, we introduced either aspartic acid or glutamic acid into the RRTRR sequence and analyzed how this exchange influenced ROS generation by Nox4. Nox4 harboring RRERR or RRDRR sequences in the B-loop was incapable of generating $H_2O_2$ (Fig. 3*B*). The RRTRR sequence is predicted to be a consensus phosphorylation site for PKC, and, thus, the exchange of threonine with glutamic acid or aspartic acid could act as a phosphomimetic Nox4 mutation. This scenario seems not to be the case, as several studies including ours indicate that treatment of Nox4 expressing cells with phorbol ester, which stimulates PKC activity, does not alter ROS generation. As observed with other B-loop mutants, all of the analyzed Nox4 mutants were similarly expressed on the cell surface (Fig. 3*C*). Sequence alignment of human Nox1–4 proteins shows that in contrast to the second pair of basic amino acids in the RRTRR motif, the first pair of basic charges is not conserved in Nox enzymes (Fig. 3*D*). This motif is unique to Nox4 and highly conserved in mammalian Nox4 enzymes, as alignment of Nox4 sequences from various species indicates (Fig. 3*E*). An upstream lysine residue (Lys-88) extends the RRTRR motif in Nox4, thus potentially forming a weak binding site for phosphatidylinositol 4,5-bisphosphate ($PI(4,5)P_2$). Negatively charged $PI(4,5)P_2$ contributes to the negative charge of the inner plasma membrane leaflet and may provide an interface that facilitates docking of Nox4 regulatory domains. ROS generation by wild-type Nox4 was analyzed after the intracellular $PI(4,5)P_2$ concentration was modulated by either coexpressing phosphatidylinositol-4-phosphate 5-kinase, which augments the $PI(4,5)P_2$ concentration, or the phosphoinositide phosphatase SopB, which hydrolyzes and thus reduces the concentration of $PI(4,5)P_2$ (18, 19). Altering the $PI(4,5)P_2$ concentration did not affect ROS generation by Nox4 (supplemental Fig. 2).

*Distinct Motifs in the C-terminal 22 Amino Acid Residues Are Essential for Nox4 Activity*—An association between Nox B-loops and their C-terminal cytosolic dehydrogenase domains has been proposed (15). Our comprehensive Nox4-Nox2 chimera screening showed earlier that replacement of the last 22 amino acids of Nox4 with residues present in Nox2 (chimera 41b) renders this chimeric enzyme non functional in respect to ROS generation without substantially altering protein expression, complex formation with p22$^{phox}$ and cell surface localization (4). Chimera 41b includes the last Nox NADPH binding domain at position 557 in Nox4 with sequence overlap in two identical amino acid residues (Fig. 4*A*). The variable residues 557–572 were analyzed for unique amino acids or motifs to pinpoint regions that may be responsible for the catalytic activity of Nox4. Exchange of the weakly positively charged histidine at position 557 to alanine (KTLAK) or serine (KTLSK) impaired ROS generation substantially (Fig. 4*B*). On the other hand, replacement of potential phosphorylation sites, Y666A and T668A, in the variable C-terminal region did not affect Nox4 activity (Fig. 4*B*). The Nox2 C-terminal sequence includes a three-amino acid insertion, directly in front of a predicted $\beta$ sheet, which may alter the distance between the B-loop and the

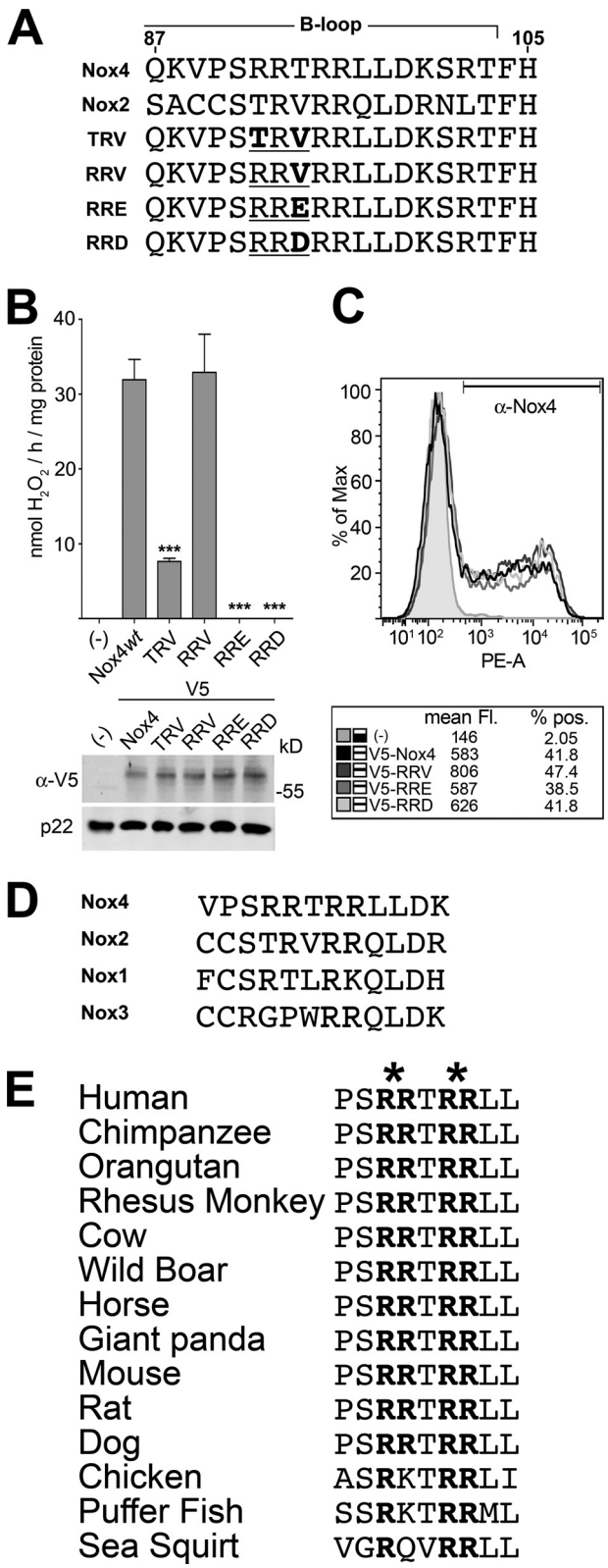


FIGURE 3. **The RRXRR motif in the B-loop is required for ROS production by Nox4.** *A*, sequence alignment of Nox4*wt*, Nox2*wt*, and the Nox4 B-loop mutants TRV, RRV, RRE and RRD. The numbers refer to the amino acid position in Nox4*wt*, and changed amino acids are highlighted in *boldface*. *B*, COS-p22$^{phox}$ cells transfected with V5-tagged Nox4*wt* or indicated Nox4 mutants were tested for $H_2O_2$ generation by HVA. The immunoblot analysis shows that expression of Nox4 proteins is comparable. p22$^{phox}$ (-) was used as a loading control. *C*, similar transfections were performed to observe Nox4 cell surface localization by flow cytometry. Cells were incubated with anti-Nox4 antibody. The fluorescence was calculated as geometric mean, and the gate was set to include 2% of control cells. COS-p22$^{phox}$ cells (-) served as a control for *B*–*C*. *D*, sequence alignment of the B-loop region containing the RR*X*RR motif of human NADPH oxidases: Nox4 (NP_058627.1), Nox2 (NP_000388), Nox1 (NP_008983), Nox3 (NP_056533). *E*, comparison of the RR*X*RR motif containing region of Nox4 proteins from different species. Accession numbers are listed under "Experimental Procedures." *Asterisks* indicate conserved amino acid residues.

dehydrogenase domain. This additional GVH sequence was inserted into the Nox4 sequence (GVHFEY) either by itself or in combination with another point mutation (GVHFIF) (Fig. 4*A*). Replacing the penultimate C terminus of Nox4 with the Nox2 C terminus or insertion of the GVH residues into Nox4 was detrimental to ROS generation by Nox4 (Fig. 4*B*), although cell surface expression was maintained (*C*). The insertion mutant was capable of producing residual $H_2O_2$, which could indicate that Nox4 residues downstream of the GVH insertion may play an additional role in providing a binding surface to transmembrane regions, including the B-loop. Nox4 contains in this region the charged polar sequence $^{571}$EY$^{572}$, which is substituted to the non polar sequence $^{564}$IF$^{565}$ in Nox2. Several Nox4 mutants were prepared to examine the importance of this sequence (Fig. 4*D*). Replacement of glutamic acid with isoleucine reduced the catalytic activity of Nox4 to ~50–60% of Nox4*wt* output, whereas the exchange of the tyrosine was inconsequential. Immunoblot analysis as well as flow cytometry confirmed comparable protein expression and plasma membrane localization of all the analyzed Nox4 mutants (Fig. 4, *D* and *E*). Comparison of the last 22 amino acids of Nox4 in mammals, birds, and fish reveal not only conservation of His-557 and Glu-571 (hNox4), but also an identical, 13-amino acid spacing of these charged residues (Fig. 4*F*), which seem to present a signature not present in any other Nox enzyme.

*The B-loop to C-terminal Interface Is Formed by Discrete Binding Sites*—The importance of charged residues in the B-loop and the C terminus of Nox4 suggests that nonspecific electrostatic effects promote the interaction between these two Nox4 domains and, ultimately, the active electron transferring conformation of the enzyme. Identification of the conserved B-loop RRTRR motif and the C-terminal FEY motif allowed the validity of this assumption to be investigated. Nox4 mutants harboring conservative substitutions of arginine with lysine and glutamic acid with aspartic acid, respectively, were prepared and compared with the Nox4 wild type in respect to ROS generation, protein expression, and cell surface localization (Fig. 5, *A*–*C*). Although the expression profiles were very similar, the KKTKK Nox4 mutant lacked catalytic activity. Replacement of glutamic acid in the FEY motif with aspartic acid (E571D) reduced ROS generation by 50% and did not rescue the activity of the KKTKK mutant when introduced into this mutant. Cell surface expression, a sign for complex formation with p22$^{phox}$ in COS-p22$^{phox}$ cells, was not disturbed in any of these Nox4 mutants (Fig. 5*C*).

*C-terminal Peptides Do Not Alter Nox4 Wild-type or Mutant Activity*—If the Nox4 C terminus domain affords direct binding to the exposed B-loop surface, this interaction should be sensitive to introduction of excess peptides derived from the C terminus of Nox4. The complete C-terminal domain ($^{304}$Nox4$^{578}$)

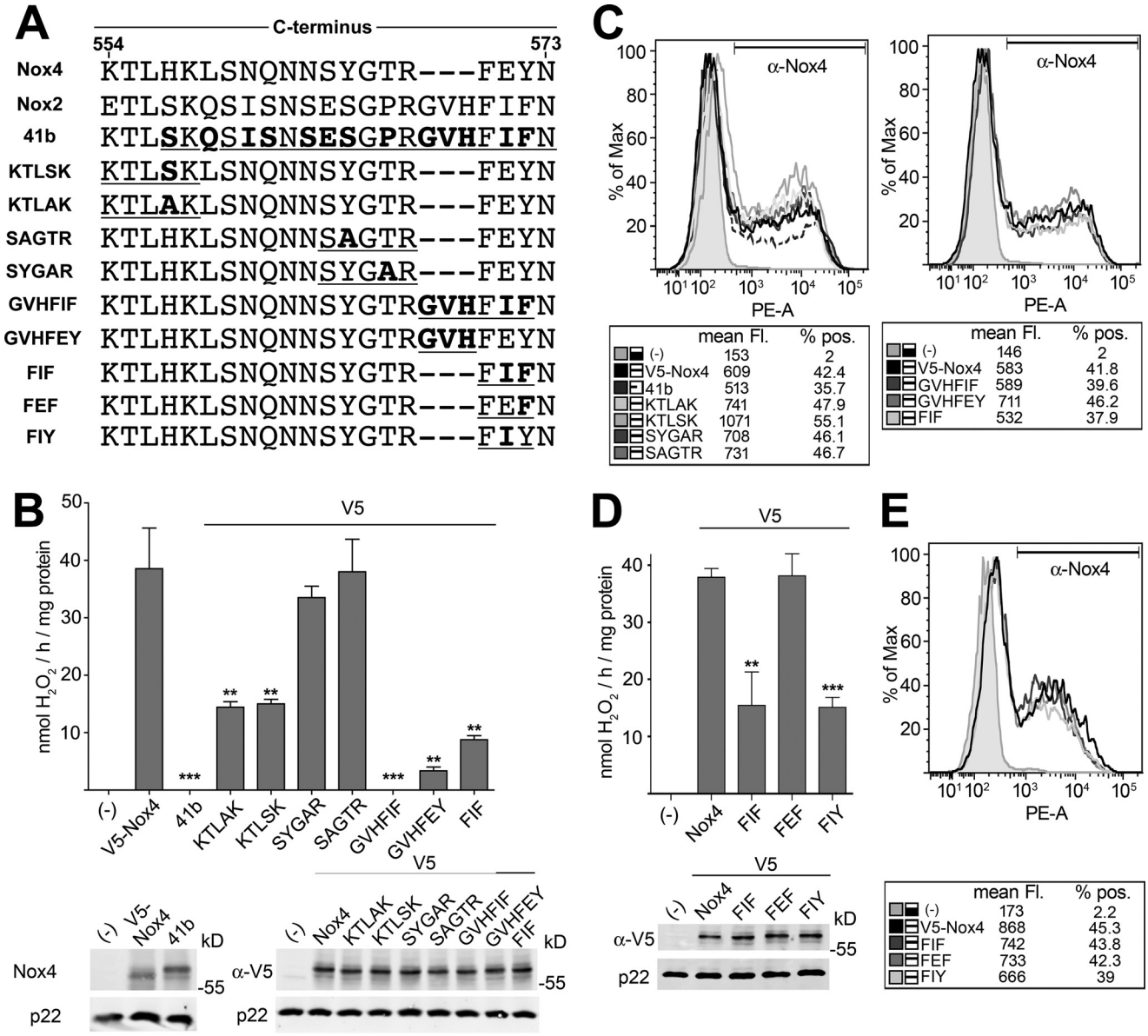
A
C-terminus
554
573
Nox4 KTLHKLSNQNNSYGTR---FEYN
Nox2 ETLSKQSISNSESGPRGVHFIFN
41b KTLSKQSISNSESGPRGVHFIFN
KTLSK KTLSKLSNQNNSYGTR---FEYN
KTLAK KTLAKLSNQNNSYGTR---FEYN
SAGTR KTLHKLSNQNNSAGTR---FEYN
SYGAR KTLHKLSNQNNSYGAR---FEYN
GVHFIF KTLHKLSNQNNSYGTRGVHFIFN
GVHFEY KTLHKLSNQNNSYGTRGVHFEYN
FIF KTLHKLSNQNNSYGTR---FIFN
FEF KTLHKLSNQNNSYGTR---FEFN
FIY KTLHKLSNQNNSYGTR---FIYN
B
nmol H2O2 / h / mg protein
V5
(-)
V5-Nox4
41b
KTLAK
KTLSK
SYGAR
SAGTR
GVHFIF
GVHFEY
FIF
Nox4
p22
α-V5
kD
-55
C
α-Nox4
% of Max
PE-A
mean Fl. % pos.
(-) 153 2
V5-Nox4 609 42.4
41b 513 35.7
KTLAK 741 47.9
KTLSK 1071 55.1
SYGAR 708 46.1
SAGTR 731 46.7
mean Fl. % pos.
(-) 146 2
V5-Nox4 583 41.8
GVHFIF 589 39.6
GVHFEY 711 46.2
FIF 532 37.9
D
nmol H2O2 / h / mg protein
V5
(-)
Nox4
FIF
FEF
FIY
α-V5
p22
kD
-55
E
α-Nox4
% of Max
PE-A
mean Fl. % pos.
(-) 173 2.2
V5-Nox4 868 45.3
FIF 742 43.8
FEF 733 42.3
FIY 666 39
F
Human LSKTLHKLSNQNNSYGTRFEYNKESFS
Chimpanzee LSKTLHKLSNQKNSYETRFEYNKESFS
Orangutan LSKTLHKLSNQINSYGTRFEYNKESFS
Rhesus Monkey LSKTLHKLSNQNNSYGTRFEYNKESFS
Cow ISKTLHKLSNRNNSYGTRFEYNKESFS
Wild Boar ISKTLHKLSNQNNSYGTRFEYNKESFS
Horse ISKTLHKLSNRNNSYGTRFEYNKESFS
Giant panda ISKTLHKLSNQNNPYGTRFEYNKESFS
Mouse ISKTLHSLSNRNNSYGTKFEYNKESFS
Rat ISKTLHNLSNRNNSYGTKFEYNKESFS
Dog ISKTLHKLSNRNNSYGTRFEYNKESFS
Chicken MSKILHKLSNSSNPYGTRFEYNKESFS
Puffer Fish ISRTLHRFCNSFQSSETVFEFNKES--
Sea Squirt LVSSVKHHCLKTKSSKVKFLFNKEAF-

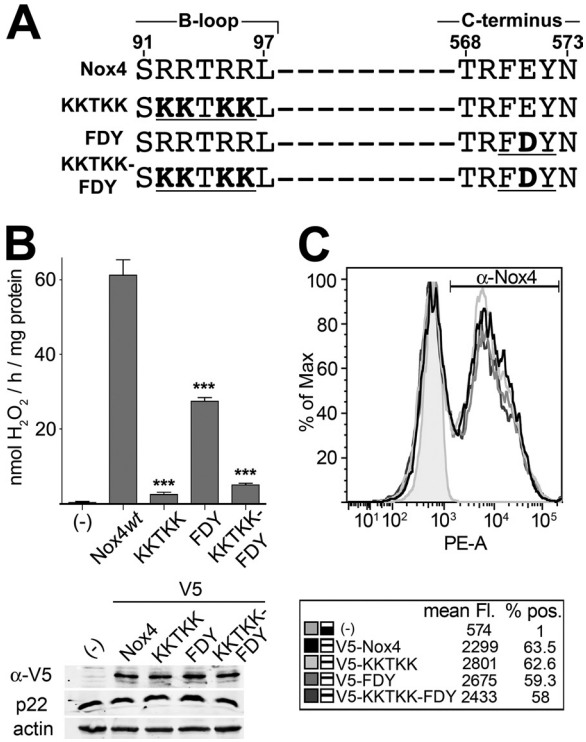


FIGURE 5. **Charged amino acids in the Nox4 B-loop and C terminus cannot be replaced by analogous residues.** *A*, sequence alignment of amino acid composition of Nox4*wt*, B-loop mutant KKTKK, C-terminal mutant FDY, and the KKTKK/FDY double mutant. The numbers refer to the amino acid position in Nox4*wt*. The *boldface* font highlights changed amino acids. *B*, COS-p22$^{phox}$ cells were transiently transfected with Nox4*wt* or indicated Nox4 mutants and tested for $H_2O_2$ generation. Expression levels of Nox4 proteins were monitored by immunoblotting using p22$^{phox}$ as a loading control. *C*, cell surface localization of Nox4 and Nox4 mutants was probed by flow cytometry. Fluorescence is calculated as geometric mean, and the gate was set to include 1% of control cells.

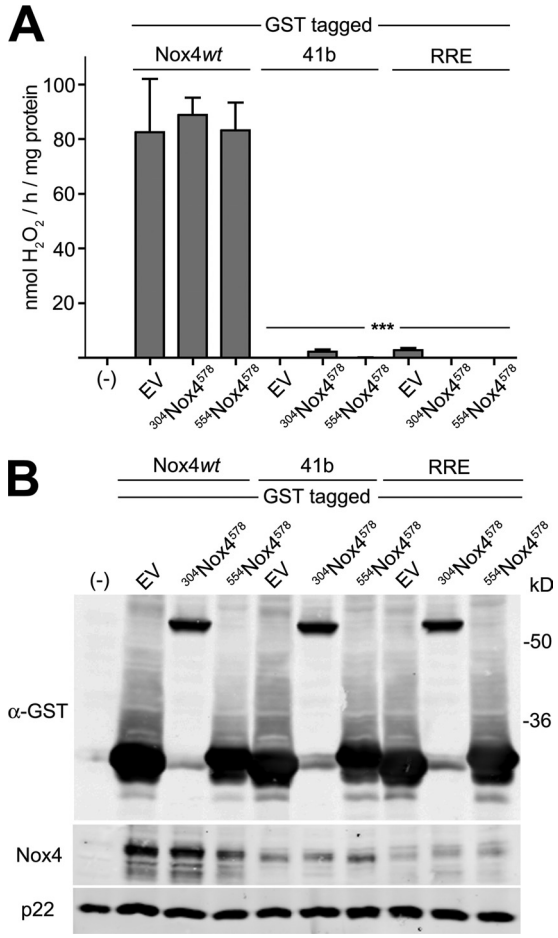


FIGURE 6. **Peptides corresponding to the C terminus of Nox4 do not interfere with Nox4*wt* activity nor rescue function of mutants 41b and RRE.** *A*, COS-p22$^{phox}$ cells were cotransfected with Nox4*wt*, Nox4/Nox2 chimera 41b, B-loop mutant RRE and indicated GST-empty vector, GST-$^{304}$Nox4$^{578}$, or GST-$^{554}$Nox4$^{578}$ and tested for $H_2O_2$ generation. *B*, expression of Nox4 and GST-tagged peptides was monitored by immunoblotting using p22$^{phox}$ as a loading control.

or the C-terminal variable domain ($^{554}$Nox4$^{578}$) were cloned into a mammalian expression vector featuring an N-terminal GST tag. These plasmids were coexpressed with the Nox4 wild type, with the Nox4-Nox2 C-terminal chimera 41b (Fig. 4), or the Nox4 B-loop mutant RRERR, both incapable of generating ROS (Fig. 3). Although the GST control peptide or the GST-tagged Nox4-derived peptides were highly expressed in COS-p22$^{phox}$ cells, inhibition of the catalytic activity of Nox4 was not detected (Fig. 6, *A* and *B*). The GST-tagged peptides failed also to rescue both catalytically inactive Nox4 mutants.

## DISCUSSION

Among the seven identified mammalian NADPH oxidases, the Nox2-based phagocyte oxidase has been extensively characterized and serves as a model system for stimulus-dependent activation of the dormant multimeric NADPH oxidase complex. Although some of the stimuli, association partners, and regulatory proteins diverge between Nox enzymes, the general process of regulating the catalytic activity of Nox is preserved. A notable exception is the constitutively active Nox4-p22$^{phox}$ complex, which seemingly generates ROS without requiring regulatory components. Nox4 provides, therefore, a simple model of a Nox enzyme in the active conformation. Previous analysis of structural elements that differ between Nox4 and other Nox enzymes has provided a wealth of information. For example, replacement of the complete Nox4 C-terminal region with the analogous region in Nox2 switches the chimeric Nox4-Nox2 enzyme to a stimulus- and regulatory component-dependent Nox, resembling the phagocyte Nox2 (4, 20). This observation reveals that assembly and activation of the multimeric Nox2-p22$^{phox}$ complex is predominantly dependent on the

FIGURE 4. **Constitutive ROS generation by Nox4 requires a charged 19-amino acid motif in the C-terminus.** *A*, sequence alignment of Nox4*wt*; Nox2*wt*; Nox4/Nox2 chimera 41b; and the Nox4 C-terminal mutants KTLSK, KTLAK, SAGTR, SYGAR, GVHFIF, GVHFEY, FIF, FEF, and FIY. Numbers refer to the amino acid position in Nox4*wt*. The *boldface* font indicates changed amino acids. *B* and *D*, COS-p22$^{phox}$ cells were transfected with V5-tagged Nox4*wt*, chimera 41b, or indicated Nox4 mutants and tested for $H_2O_2$ generation. Immunoblot analyses showing expression of Nox4 proteins are comparable using anti-Nox4 or anti-V5 tag antibodies. p22$^{phox}$ was used as a loading control. *C* and *E*, COS-p22$^{phox}$ cells were transfected in a similar fashion to verify cell surface localization of Nox4 proteins by flow cytometry. Fluorescence is calculated as geometric mean, and the gate was set to include 2% of control cells. COS-p22$^{phox}$ cells (-) served as a control. *F*, comparison of the last 27 amino acids of the C terminus of Nox4 proteins from different species. The accession numbers are listed under "Experimental Procedures." *Asterisks* indicate conserved amino acid residues.

Nox2 C terminus in conjunction with $p22^{phox}$. The ability to generate ROS was comparable in Nox4-Nox2 (C-terminal) chimeras containing their cognate or a Nox4 chimeric B-loop (4), indicating that the Nox4 B-loop provides sufficient interaction sites for Nox2 regulatory components such as $p47^{phox}$ or for an intramolecular interaction with the Nox2 dehydrogenase domain. An analogous Nox2-Nox4 chimera was expressed but not functional in adherent COS-$p22^{phox}$ cells (4). Nisimoto *et al.* (20) reported reduced, but constitutive activity of a similar chimera that contained an upstream extension of the Nox4 C terminus by four amino acids ($^{300}$YRYI$^{303}$) when analyzing transfected HEK293 cells in suspension. Expression of this chimera in our cellular system, which depends on cell adherence and plasma membrane localization of Nox4, did not lead to $H_2O_2$ production (supplemental Fig. 3). Even matching the Nox4 C terminus with its cognate B-loop in a Nox2-Nox4 chimera did not rescue catalytic activity (4), suggesting that structural hindrance imposed by the Nox2 backbone may impede proper folding. A possible explanation for discrepancy in observations could lie in the spatial restrictions imposed on the Nox complex during cell attachment or in suspension-induced translocation of yet unknown Nox4-associated signaling molecules in the HEK293 cell type.

The constitutive activity of exogenously expressed Nox4 requires only the $p22^{phox}$ subunit. One can speculate that the assembly of the Nox4-$p22^{phox}$ heterodimer differs from that of the Nox2-$p22^{phox}$ heterodimer. The unique tertiary structure of the Nox4-$p22^{phox}$ complex may permit constitutive electron transfer from NADPH to FAD and the hemes. In every published expression system, the Nox4 complex appears locked into this conformation and thus remains active. We show here that multiple residues in the B-loop and in the last C-terminal 22 amino acid residues are critical for the catalytic activity of Nox4. Replacement of amino acids in the Nox4 B-loop, either in rather conserved regions or in the variable domain, with amino acids matching the Nox2 sequence reduced Nox4 activity considerably. Introduction of negative charge into clustered positively charged motifs such as the $^{92}$RRxRR$^{96}$ or the $^{100}$KxR$^{102}$ motif abolished ROS generation. We identified an RR*X*RR motif in mammalian Nox4 enzymes, which provides not only electrostatic charge but also a specific binding site for either unknown binding partners or for the dehydrogenase domain. The second set of arginine residues in the RR*X*RR motif is known to be important for Nox2 and Nox4 activity (9, 15), whereas the first set of arginines is only present in Nox4. Single replacement of arginine with non-polar valine in position 93 in Nox4 seems not to disrupt the B-loop interaction surface (15), whereas substitution of the complete arginine B-loop motif with lysines (KK*X*KK), featuring a comparable positive charge, rendered Nox4 non-functional. Although the charge and size of the amino acids arginine and lysine are similar, many enzymes do not tolerate arginine substitution in their active site (21). The rigid geometry of the arginine guanidinium group and potential arginine-phosphoryl interactions have been proposed as a basis for arginine specificity. Although arginine residues also dominate in the variable region of the B-loops of Nox1–3, replacement of one of those residues with lysine, as it occurs in the Nox1 sequence, seems to be inconsequential. Further observations that several amino acid residues, independently of their charge, cannot be exchanged without substantially reducing ROS generation, points to the B-loop as a highly sensitive region required for the catalytic activity of Nox4.

Most lipid-binding domains characterized so far are found to be ~50–150 amino acids in length. Nevertheless, smaller stretches of basic amino acids can act as phosphoinositide binding sites and could contribute to protein targeting or stabilize the spatial structure of proteins attached to membranes in a nonspecific manner. Anionic lipids play an important role in Nox2 complex assembly and activation and could potentially interact directly with the polybasic Nox4 B-loop. Modulation of intracellular $PI(4,5)P_2$ levels did not alter ROS generation by Nox4, a result that is consistent with our mutational analysis as $PI(4,5)P_2$ would not show such distinct preference for arginine residues. This result supports the notion that the B-loop contains a discrete binding site for either internal Nox4 domains or yet uncharacterized interaction partners.

The current model for Nox activation postulates binding of Nox C-terminal domains to the B-loop when Nox enzymes assume their active state. A recent study using recombinant GST-fusion proteins encompassing fragments of the Nox4 dehydrogenase domain in conjunction with labeled B-loop peptides determined amino acid residues 420–488 in Nox4 as potential binding region (15). In contrast, we identified a C-terminal region further downstream, just after the second NADPH binding motif, as crucial for Nox4, but not Nox2 catalytic activity in cell culture studies (chimera 11b and 11a) (4). This region was further limited to the last 22 amino acids of Nox4 (chimera 41b). Substitution of unique amino acid residues in this short region, such as His-557 or Glu-571, decreased ROS generation substantially, whereas exchange of two potential phosphorylation sites did not alter Nox4 activity. Nox2 and the related Nox1 and Nox3 enzymes contain a three-amino acid insertion in the penultimate C terminus (GVH in Nox2 and Nox3, KVQ in Nox1). Introducing the Nox2 sequence GVH into Nox4 was not tolerated and markedly reduced ROS generation. In conclusion, the absence of catalytic activity of the $^{1}$Nox4$^{556/547}$Nox2$^{570}$chimera (41b) is caused by several unique features that may influence interaction and/or distance between the dehydrogenase domain and B-loop. Of note, Nox4 also lacks another insert, a sequence located directly in front of the chimera 11 substitution site. This Nox2 sequence, encompassing amino acids 484–504, which is substantially shorter in Nox4, has been implicated in maintaining the inactive state of the enzyme (22). Together with the missing GVH insert, these changes alter the overall distance between FAD and NADPH binding regions and the conserved, critical C-terminal residue Phe-577. This structural difference may permit the Nox4 but not the Nox1–3 dehydrogenase domain to fold into closer proximity to the transmembrane loops without the assistance of additional cofactors, thereby connecting those regions.

Inhibition of Nox2 or Nox4 catalytic activity by cognate B-loop derived peptides *in vitro* and the observation that $X^+$ CGD mutations in the second transmembrane domain of Nox2, which is situated just upstream of the B-loop, alter diaphorase activity, indicate that Nox B-loops constitute an essential part of the electron transfer machinery (14, 15, 23).

Although the Nox2 B-loop may provide a p47$^{phox}$ binding site, an analogous protein partner has not been identified for Nox4. If the constitutive activity of Nox4 were caused solely by high-affinity binding of the dehydrogenase domain to the B-loop, one would expect that excess of C-terminal peptide would disrupt this interaction and would lead to reduced ROS generation. Expression of fusion proteins encompassing either the full-length Nox4 C terminus or the terminal 22 amino acids in COS-p22$^{phox}$ cells expressing constitutively active Nox4, did not affect ROS output. One possible explanation could be inaccessibility of the rather bulky hydrophilic peptide to the membrane compartment harboring the Nox4-p22$^{phox}$ complex, whereas a polybasic minimal B-loop peptide may gain access. More likely, the Nox4-p22$^{phox}$ complex may assemble in the endoplasmic reticulum in an enzymatically active conformation that will be transported to the plasma membrane or other intracellular locations as such. This notion is supported by the observation that in some cell types constitutively active Nox4-p22$^{phox}$ heterodimers can be localized in endoplasmic reticulum-associated vesicular structures. In COS-p22$^{phox}$ cells, failure to dimerize with p22$^{phox}$ leads to accumulation of inactive Nox4 in the endoplasmic reticulum, whereas all Nox4 mutants or Nox4-Nox2 chimeras that form catalytically inactive Nox4-p22$^{phox}$ complexes because of defects in the electron transport localize to the plasma membrane. Activity of Nox4 complexes is always accompanied by maturation to the cell surface in this cell type.

Structure-function analysis of the active conformation of Nox enzymes is a prerequisite for development of selective inhibitors targeting only one particular Nox isoform. Currently available compounds are either not selective, for example GKT 136901, or of limited bioavailability *in vivo* (Nox2ds-Tat) or possess considerable unspecific toxicity when tested in cell culture (Nox4ds-Tat) (24). Although the Nox4 B-loop may provide a potential target for drug design, *in vivo* selectivity might be hard to achieve. Development of small peptides disrupting Nox4 dehydrogenase domain folding in the ER or identification of small molecules that disrupt the discrete binding site provided by the RR*X*RR B-loop motif could be a first step toward selective inhibitors for Nox4.

## REFERENCES


1. Bedard, K., and Krause, K. H. (2007) The NOX family of ROS-generating NADPH oxidases. Physiology and pathophysiology. *Physiol. Rev.* **87,** 245–313
2. Kawahara, T., Quinn, M. T., and Lambeth, J. D. (2007) Molecular evolution of the reactive oxygen-generating NADPH oxidase (Nox/Duox) family of enzymes. *BMC Evol. Biol.* **7,** 109
3. Sumimoto, H. (2008) Structure, regulation and evolution of Nox-family NADPH oxidases that produce reactive oxygen species. *FEBS J.* **275,** 3249–3277
4. von Löhneysen, K., Noack, D., Wood, M. R., Friedman, J. S., and Knaus, U. G. (2010) Structural insights into Nox4 and Nox2. Motifs involved in function and cellular localization. *Mol. Cell. Biol.* **30,** 961–975
5. Takac, I., Schröder, K., Zhang, L., Lardy, B., Anilkumar, N., Lambeth, J. D., Shah, A. M., Morel, F., and Brandes, R. P. (2011) The E-loop is involved in hydrogen peroxide formation by the NADPH oxidase Nox4. *J. Biol. Chem.* **286,** 13304–13313
6. Martyn, K. D., Frederick, L. M., von Loehneysen, K., Dinauer, M. C., and Knaus, U. G. (2006) Functional analysis of Nox4 reveals unique characteristics compared to other NADPH oxidases. *Cell. Signal.* **18,** 69–82
7. Park, M. Y., Imajoh-Ohmi, S., Nunoi, H., and Kanegasaki, S. (1997) Synthetic peptides corresponding to various hydrophilic regions of the large subunit of cytochrome b558 inhibit superoxide generation in a cell-free system from neutrophils. *Biochem. Biophys. Res. Commun.* **234,** 531–536
8. DeLeo, F. R., Yu, L., Burritt, J. B., Loetterle, L. R., Bond, C. W., Jesaitis, A. J., and Quinn, M. T. (1995) Mapping sites of interaction of p47-phox and flavocytochrome b with random-sequence peptide phage display libraries. *Proc. Natl. Acad. Sci. U.S.A.* **92,** 7110–7114
9. Biberstine-Kinkade, K. J., Yu, L., and Dinauer, M. C. (1999) Mutagenesis of an arginine- and lysine-rich domain in the gp91(phox) subunit of the phagocyte NADPH-oxidase flavocytochrome b558. *J. Biol. Chem.* **274,** 10451–10457
10. Rey, F. E., Cifuentes, M. E., Kiarash, A., Quinn, M. T., and Pagano, P. J. (2001) Novel competitive inhibitor of NAD(P)H oxidase assembly attenuates vascular O(2)(-) and systolic blood pressure in mice. *Circ. Res.* **89,** 408–414
11. Liu, J., Yang, F., Yang, X. P., Jankowski, M., and Pagano, P. J. (2003) NAD(P)H oxidase mediates angiotensin II-induced vascular macrophage infiltration and medial hypertrophy. *Arterioscler. Thromb. Vasc. Biol.* **23,** 776–782
12. Al-Shabrawey, M., Bartoli, M., El-Remessy, A. B., Platt, D. H., Matragoon, S., Behzadian, M. A., Caldwell, R. W., and Caldwell, R. B. (2005) Inhibition of NAD(P)H oxidase activity blocks vascular endothelial growth factor overexpression and neovascularization during ischemic retinopathy. *Am. J. Pathol.* **167,** 599–607
13. Zhou, X., Bohlen, H. G., Miller, S. J., and Unthank, J. L. (2008) NAD(P)H oxidase-derived peroxide mediates elevated basal and impaired flow-induced NO production in SHR mesenteric arteries *in vivo*. *Am. J. Physiol. Heart Circ. Physiol.* **295,** H1008-H1016
14. Csányi, G., Cifuentes-Pagano, E., Al Ghouleh, I., Ranayhossaini, D. J., Egaña, L., Lopes, L. R., Jackson, H. M., Kelley, E. E., and Pagano, P. J. (2011) Nox2 B-loop peptide, Nox2ds, specifically inhibits the NADPH oxidase Nox2. *Free Radic. Biol. Med.* **51,** 1116–1125
15. Jackson, H. M., Kawahara, T., Nisimoto, Y., Smith, S. M., and Lambeth, J. D. (2010) Nox4 B-loop creates an interface between the transmembrane and dehydrogenase domains. *J. Biol. Chem.* **285,** 10281–10290
16. Yu, L., Zhen, L., and Dinauer, M. C. (1997) Biosynthesis of the phagocyte NADPH oxidase cytochrome b558. Role of heme incorporation and heterodimer formation in maturation and stability of gp91phox and p22phox subunits. *J. Biol. Chem.* **272,** 27288–27294
17. von Löhneysen, K., Noack, D., Jesaitis, A. J., Dinauer, M. C., and Knaus, U. G. (2008) Mutational analysis reveals distinct features of the Nox4-p22 phox complex. *J. Biol. Chem.* **283,** 35273–35282
18. Coppolino, M. G., Dierckman, R., Loijens, J., Collins, R. F., Pouladi, M., Jongstra-Bilen, J., Schreiber, A. D., Trimble, W. S., Anderson, R., and Grinstein, S. (2002) Inhibition of phosphatidylinositol-4-phosphate 5-kinase I$\alpha$ impairs localized actin remodeling and suppresses phagocytosis. *J. Biol. Chem.* **277,** 43849–43857
19. Hernandez, L. D., Hueffer, K., Wenk, M. R., and Galán, J. E. (2004) *Salmonella* modulates vesicular traffic by altering phosphoinositide metabolism. *Science* **304,** 1805–1807
20. Nisimoto, Y., Jackson, H. M., Ogawa, H., Kawahara, T., and Lambeth, J. D. (2010) Constitutive NADPH-dependent electron transferase activity of the Nox4 dehydrogenase domain. *Biochemistry* **49,** 2433–2442
21. Gorrell, A., Lawrence, S. H., and Ferry, J. G. (2005) Structural and kinetic analyses of arginine residues in the active site of the acetate kinase from *Methanosarcina thermophila*. *J. Biol. Chem.* **280,** 10731–10742
22. Taylor, W. R., Jones, D. T., and Segal, A. W. (1993) A structural model for the nucleotide binding domains of the flavocytochrome b-245 $\beta$-chain. *Protein Sci.* **2,** 1675–1685
23. Picciocchi, A., Debeurme, F., Beaumel, S., Dagher, M. C., Grunwald, D., Jesaitis, A. J., and Stasia, M. J. (2011) Role of putative second transmembrane region of Nox2 protein in the structural stability and electron transfer of the phagocytic NADPH oxidase. *J. Biol. Chem.* **286,** 28357–28369
24. Lambeth, J. D., Krause, K. H., and Clark, R. A. (2008) NOX enzymes as novel targets for drug development. *Semin. Immunopathol.* **30,** 339–363